THE ASTROPHYSICAL JOURNAL, 190:73–83, 1974 May 15

THE NATURE OF INFRARED EXCESSES IN EXTREME Be STARS

RUDOLPH SCHILD, FREDERIC CHAFFEE, JAY A. FROGEL, AND S. ERIC PERSSON
Center for Astrophysics, Harvard College Observatory and Smithsonian Astrophysical Observatory
Received 1973 July 18

ABSTRACT

Newly measured energy distributions from 0.32–3.5 μ for all the extreme Be stars around χ Per show an infrared excess beginning at 0.5 μ, peaking shortward of 1 μ, and declining at longer wavelengths. This excess is not likely to be thermal radiation from dust, but appears to be continuum radiation from the free-bound electron interaction with neutral hydrogen. The emission presumably originates in a large gas shell around the extreme Be stars.

The H-R diagrams for four clusters containing extreme Be stars are consistent with the hypothesis that the extreme Be stars are in the core-contraction stage of post–main-sequence evolution, following exhaustion of hydrogen in their convective cores. The possible role of resonance absorption in providing pressure support for the very large extreme Be star shells is noted.

The eight extreme Be stars observed to date are found to have continuous or nearly continuous energy distributions across the Balmer jump. None appears to have a Balmer discontinuity in emission. One star varied by 0.3 mag at 1.6 and 2.2 μ, and a second appears to have varied by 0.1 mag, on a time scale of 1 year.

Subject headings: Be stars — circumstellar shells — infrared

I. INTRODUCTION

The study of Be stars is hampered by the diversity of objects under study and by the wide range of phenomena exhibited by individual stars. Irregular variations of brightness, emission line strength, infrared excesses, and radial velocity of the absorption and emission line spectra are documented to varying degrees for a large number of stars. Because of the anomalous colors shown by many Be stars owing to excess emission shortward of the Balmer discontinuity and in the Paschen continuum and infrared, it is difficult, as discussed below, to derive distances, reddening, and effective temperatures of individual stars.

Several classes of Be stars have been identified. The *supergiants* frequently show emission at Hα, and the highest luminosity objects may show P Cyg emission profiles in other lines as well; however, hydrogen emission is apparently not primarily a rotation effect in the stars of highest luminosity, and supergiants will not be considered further in this paper. The *shell stars* tend to be spectrum variables that, at time of peak activity, are surrounded by a thick shell of gas that replaces the absorption spectrum of the quiescent star by a lower excitation spectrum characterized by very sharp lines. The *pole-on stars* were identified as objects with sharp emission lines superposed on broad, shallow absorption components and with relatively sharp He I absorption lines; the interpretation that these are ordinary Be stars viewed along their axes of rotation, with sharp He I lines due to low line-of-sight velocities and broad hydrogen absorptions due to the pressure-temperature structure of the star's polar regions, has been questioned by Schild (1972), who has noted that, with regard to the strength and permanence of the emission lines and the infrared excesses, the pole-on stars are atypical Be stars in a way not readily understood as an orientation effect. A final group of Be stars, identified on the basis of spectroscopic criteria, now called simply *extreme Be stars* and previously identified as objects in the core-contraction phase subsequent to the exhaustion of hydrogen in the convective cores, has been recognized in the h and χ Per association by Schild (1966), who has also noted the spectroscopic similarity of the extreme Be stars to the pole-on stars. The great majority of Be stars belong to none of the above classes but are spectroscopically very similar to normal B stars except for the occasional appearance of emission in the hydrogen lines.

The purpose of the present paper is to specify further the properties of the extreme Be stars, particularly with regard to their continuous energy distributions, and to strengthen the previously noted connection with the pole-on stars and the core-contraction stage of post–main-sequence evolution.

We begin with some remarks about the current picture of the evolution of rotating stars. The most recent stellar-model calculations by Sackmann and Anand (1970) confirm the earlier work by Crampin and Hoyle (1960), which showed that all but the slowest rotators will have a serious excess of angular momentum at the stage of secondary core contraction and that many rapid rotators will also be Be stars in their early evolution off the main sequence. It is also important that the stars reaching the core-contraction stage will have been made similar to one another by forced rotational ejection; the most rapidly rotating stars will lose angular momentum in early post–main-sequence evolution, whereas less rapid rotators begin losing mass later in their evolution but still before core contraction. Thus, we would expect a substantial fraction of stars to enter the secondary core-contraction stage with comparable amounts of angular momentum.

From this picture, we would expect the Be stars in secondary core contraction to be relatively homogeneous in their observable properties and to manifest

strongly the Be phenomena. On this basis, the χ Per extreme Be stars were first identified as core-contraction stars by Schild (1966), who also noted other confirming evidence such as the location in the H-R diagram. Further, the spectroscopic similarity to the pole-on stars was noted. The pole-on stars were investigated by Schild (1973), who found them to be probable core-contraction stars on the basis of the strength and permanence of their hydrogen and infrared emission, although nothing has been established about their evolutionary status from cluster H-R diagrams, since all are field stars (except χ Oph, discussed in § V).

In the study of continuum energy distributions of Be stars, it is particularly useful to concentrate on cluster stars because, as will be seen below, the energy distributions are so peculiar that interstellar reddening effects can be estimated only by referring to the reddening of nearby cluster members. The young galactic cluster χ Per is a very favorable case for study, because it contains a significant number of ordinary Be stars as well as eight extreme Be stars in the cluster nucleus and surrounding region. The ages, distances, reddening, and evolutionary states of the several classes of Be stars are reasonably well known in the χ Per region.

A previous study based on continuum energy distributions $\lambda\lambda$3500–6000, as well as infrared photometry, for three extreme Be stars in the region around χ Per showed all three to have large infrared excesses beginning in the 5000 Å region (Schild 1972). It was pointed out that these excesses could not be understood as thermal emission from a dust cloud; instead, the excess was described as continuum radiation from the envelopes surrounding the three stars. It was further noted that this excess continuum radiation could explain several of the properties of the extreme Be stars noted by Schild (1966): (*a*) The unusual redness of the extreme Be stars is explained by the contributions of the excess radiation in the V bandpass. (*b*) The veiling of the absorption lines could be understood as resulting from filling in by the excess continuum radiation. (*c*) The Fe II and H emission lines observed would naturally arise in a shell of moderate temperature and low density.

Since relatively little is known to date about continuous energy distributions of ordinary Be stars, we present in Appendix A a discussion of the relation between the Paschen continuum slope and the Balmer discontinuity, together with spectral types, of 10 ordinary Be stars. We find that most Be stars show the normal relation between spectral type, Paschen continuum slope, and Balmer discontinuity. However, a few ordinary Be stars have abnormally small Balmer discontinuities. None of the ordinary Be stars, however, shows the near-infrared excess typical of the Perseus extreme Be stars (discussed below).

II. OBSERVATIONS

New observations were made of all the extreme Be stars in the χ Per region; the new energy distributions were measured from $\lambda\lambda$3200–8000 (50 Å bandpass) during 1971 October 18–24, and new infrared photometry was obtained on 1972 January 10 at 1.6, 2.2, and 3.5 μ. All observations were made with the 60-inch (1.5-m) Tillinghast reflector at Mount Hopkins Observatory. The new magnitudes, uncorrected for reddening, are listed in table 1. The optical and infrared fluxes are on the systems of absolute calibration by Oke and Schild (1970), and Wilson *et al.* (1972), respectively. The scanner observations produced color data only, which were put on the magnitude system by adopting the V magnitude given by Schild (1966) as the λ5556 flux; this would cause a mismatch with the infrared data if the stars have varied in brightness since 1966. Dates of observation for visual and infrared data are given in Appendix B. The rms deviations of the infrared photometry were less than the systematic errors, taken to be 0.05 mag at 1.6 and 2.2 μ, except for the 3.5-μ data for which 1 σ errors are listed in table 1.

The new data were corrected for reddening by using a map of the color excesses of nearby OB stars in the h and χ Per association. This was necessary because, as noted by Schild (1966), the extreme Be stars show an anomalously large $B - V$ excess that is apparently not a result of interstellar reddening. The stars were dereddened by using the Perseus interstellar reddening law of Whiteoak (1966). Because that law extends only to λ3450, the curve was extended to λ3200 by a procedure described in Appendix C. The dereddened energy distributions are shown in figure 1, where each is compared with the dereddened energy distribution of a star of comparable temperature, luminosity, and age (HD 13900).

III. BALMER DISCONTINUITIES OF EXTREME Be STARS

Two features of the energy distributions of extreme Be stars are immediately evident: All have large excesses of radiation shortward of the Balmer discontinuity and in the infrared. The ultraviolet data seem to show that at the shortest wavelengths (λ3200) the extreme Be stars have about the same flux relative to 4000 Å as does the normal giant HD 13900, but that the Balmer continuum near the Balmer discontinuity is filled in for the extreme Be stars. It may be particularly significant in this regard that none of the extreme Be stars has its Balmer discontinuity in emission and that the stars with the strongest infrared excesses (HD 14605, MWC 449, MWC 448) appear to have continuous energy distributions across the Balmer discontinuity. Since the same absolute calibration and reddening law were used in the comparison of the extreme Be stars with HD 13900, the character of the continuum across the Balmer discontinuity is not likely to be an artifact of the data-handling procedures.

IV. THE INFRARED EXCESSES OF EXTREME Be STARS

The infrared excesses are surprisingly similar with regard both to the wavelength at which the excess is first apparent and the amount of the excess. The

TABLE 1

ENERGY DISTRIBUTIONS OF EXTREME Be STARS

λ (Å)	ν (10^{14} Hz)	HD 14422	HD 14605	Hi 263	MWC 43	MWC 445	MWC 448	MWC 449	Oo 2284
3200.....	9.38	9.83	9.71	10.15	11.09	10.06	12.19	11.80	10.50
3250.....	9.23	9.79	9.66	10.12	11.03	10.00	12.15	11.74	10.45
3300.....	9.09	9.75	9.60	10.06	10.98	9.93	12.05	11.66	10.40
3350.....	8.96	9.72	9.60	10.06	10.99	9.91	12.01	11.55	10.38
3400.....	8.82	9.68	9.52	10.01	10.83	9.87	11.95	11.58	10.32
3450.....	8.70	9.65	9.45	10.01	10.79	9.83	11.91	11.53	10.26
3500.....	8.57	9.62	9.45	9.98	10.77	9.81	11.87	11.51	10.28
3571.....	8.40	9.61	9.45	9.99	10.75	9.81	11.84	11.48	10.26
3636.....	8.25	9.58	9.43	9.97	10.69	9.78	11.78	11.44	10.25
1036.....	7.43	9.40	9.48	9.86	10.53	9.66	11.61	11.28	10.05
4167.....	7.20	9.37	9.49	9.84	10.49	9.63	11.56	11.23	10.03
4255.....	7.05	9.35	9.51	9.84	10.47	9.62	11.55	11.20	10.02
4464.....	6.72	9.29	9.47	9.80	10.40	9.56	11.46	11.13	9.96
4566.....	6.57	9.28	9.47	9.79	10.36	9.57	11.42	11.08	9.94
4785.....	6.27	9.23	9.48	9.79	10.30	9.53	11.35	11.02	9.91
5000.....	6.00	9.16	9.44	9.74	10.20	9.48	11.23	10.90	9.83
5263.....	5.70	9.06	9.38	9.68	10.03	9.39	11.02	10.68	9.74
5556.....	5.40	8.99	9.34	9.63	9.91	9.30	10.88	10.58	9.66
5840.....	5.14	8.99	9.37	9.61	9.90	9.32	10.87	10.52	9.68
6056.....	4.95	8.97	9.37	9.62	9.86	9.30	10.80	10.49	9.65
6436.....	4.66	8.96	9.35	9.58	9.79	9.26	10.73	10.39	9.58
6790.....	4.42	8.91	9.34	9.56	9.71	9.23	10.65	10.33	9.55
7100.....	4.23	8.89	9.30	9.54	9.68	9.19	10.57	10.25	9.51
7550.....	3.97	8.86	9.28	9.49	9.59	9.14	10.47	10.19	9.44
7780.....	3.85	8.82	9.22	9.47	9.51	9.06	...	10.09	9.37
8090.....	3.71	8.80	9.19	...	...	9.06	...	...	9.34
1.6 μ	1.88	8.30	8.47	8.48	8.50	8.38	9.24:	...	8.26
2.2 μ	1.36	8.12	8.18	8.22	8.07	8.04	9.28	...	7.98
3.5 μ	0.86	7.82	8.11	...	7.80	7.61	...	...	7.22
$\pm\sigma(3.5)$...	...	$\pm$0.13	$\pm$0.33	...	$\pm$0.14	$\pm$0.15	...	...	$\pm$0.16
E_{B-V}.....	...	0.57	0.32	0.42	0.65	0.52	0.70	0.70	0.59

excesses are not artifacts of the reddening correction made, since the amounts of reddening required to obtain favorable comparisons with the continuum of HD 13900 are inadmissibly large, especially for Oo 2284, which lies in χ Per, where reddening has been found by Crawford, Glaspey, and Perry (1970) to be uniform. Moreover, applying larger reddening corrections to fit the 4000–6000 Å region produces energy distributions that sag at 5000 Å but nevertheless have infrared excesses. Although the possibility of circumstellar reddening cannot be ruled out, it would be surprising if such reddening were of just the right amount and had the right wavelength dependence to produce continuous energy distributions across the Balmer discontinuity.

The infrared excesses may have an explanation in the recent theoretical work of Milkey and Dyck (1973). These authors have computed the expected free-free emission from an isothermal shell surrounding a hot star and compared their predicted energy distributions with broad-band photometry of several Be stars. They conclude that cool (T_e = 3000° K) free-free emission is more attractive for explaining infrared excesses in Ae and Be stars than is the thermal dust emission. Unfortunately, their observed energy distributions do not show the broad emission feature centered at approximately 1 μ, which is characteristic of the free-bound opacity of electrons with H, and they conclude that electron-hydrogen free-free emission is not dominant in the Be star shells.

The present observations of extreme Be stars show a feature in the near-infrared similar to that expected from the H^- free-bound continuum. Figures 2*a* and 2*b* show the observed energy distributions of the infrared excesses, obtained by subtracting from the dereddened fluxes of the eight extreme Be stars the measured continuum flux of HD 13900, normalized in the 4000 Å region. Also shown is the normalized contribution to the continuum predicted by Milkey and Dyck (1973) for an isothermal shell of temperature T_e = 3000° K. The following features of the graph are immediately recognized:

a) The curves for the eight stars are similar, particularly with respect to the wavelength at which the excesses are first observed in the visible and the manner in which they cut off in the infrared. This suggests that the reddening corrections are probably valid.

b) The total strengths for the eight stars vary by a factor less than 3, a striking result. This is consistent with the remark by Schild (1966) that the spectra look very similar.

c) The wavelength at which the theoretical curve peaks is about 3000 Å too far to the red, but this is not considered an important discrepancy, because no attempt has yet been made to vary the shell parameters, particularly the temperature, to give agreement. The data presented in § V (see fig. 3) show that the wavelength of the maximum is different for NGC 6530 No. 65, so the details of the energy distribution of the

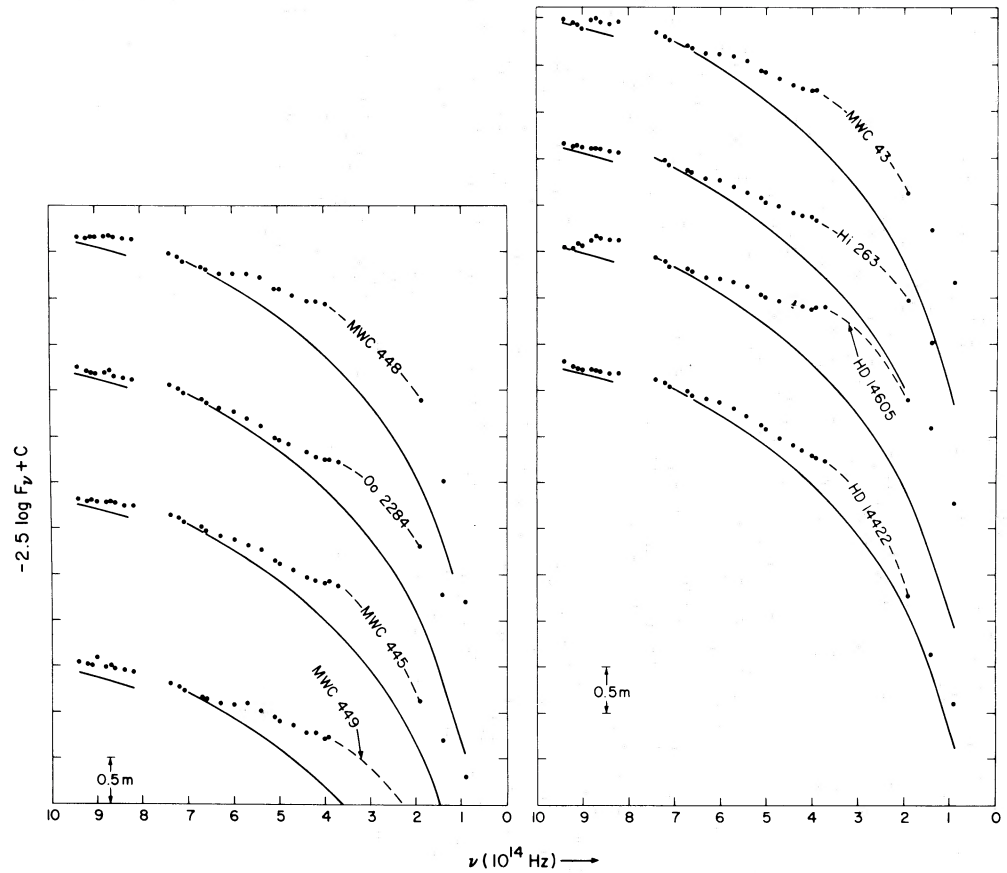

FIG. 1.—Energy distributions of extreme Be stars in the region of χ Per, compared to the dereddened continuum of HD 13900 (B1 III). All energy distributions have been dereddened according to procedures described in § II. Dates of observation for the visible and infrared data are given in Appendix A. Particularly interesting is the tendency of many of the infrared excesses to *decline* at longer wavelengths.

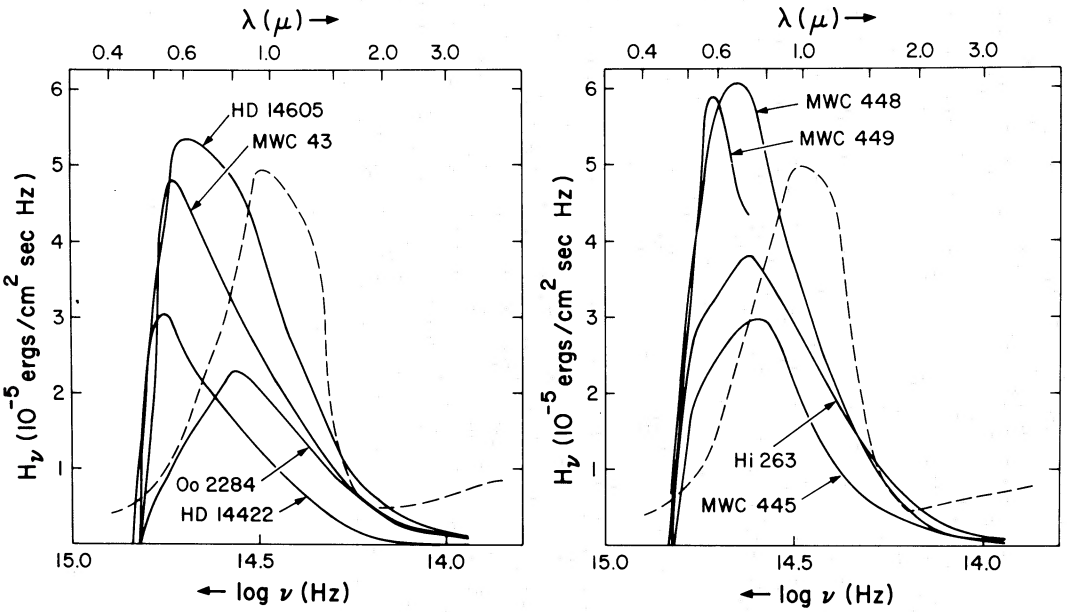

FIG. 2.—Infrared excesses of the extreme Be stars, smoothed and plotted in absolute units on a linear intensity scale. The theoretical H^- bound-free energy distribution for $T_e = 3000°$ K and arbitrary normalization is shown as the dashed curve.

TABLE 2

INFRARED EXCESS IN Hi 263

λ (Å)	log ν	ΔF_ν (10^{-5} ergs s^{-1} cm^{-2} Hz^{-1})
4464	14.83	0.7
4566	14.82	0.8
4785	14.80	1.4
5000	14.78	2.9
5263	14.76	2.6
5556	14.73	3.2
5840	14.71	3.0
6056	14.69	3.6
6436	14.67	2.9
6790	14.64	4.0
7100	14.63	3.3
7550	14.60	3.9
7780	14.59	3.7
1.6 μ	14.26	0.9
2.2 μ	14.13	0.4
3.5 μ	13.94	0.1

excess radiation must depend on the shell parameters. Calculations are about to be made with a model-atmosphere program that will compute the shell emission as a function of electron temperature and density.

d) The low-frequency part of the theoretical curve begins to increase because of the contribution of the H^- free-free emission, which is also included in Milkey and Dyck's calculations. Since the ratio of free-bound to free-free emission is also temperature and density dependent, more adjustment of parameters may give a better fit at the long wavelengths.

In many respects, Hi 263 appears to have an "average" infrared excess for the eight stars. We list in table 2 the unsmoothed excess for Hi 263 for others who might wish to fit it to models.

The total power emitted in the H^- free-bound continuum, integrated over all frequencies, is given in table 3. The value of $\int H_\nu d\nu$ was derived by integrating the continuum excesses of figure 2 and adopting the Eddington flux at λ5556 of 2.21×10^{-4} ergs s^{-1} cm^{-2} sr^{-1} Hz^{-1} from Mihalas's (1972, table 2) $T_{\rm eff}$ = 25,000° K, log g = 3.0, non-LTE (NLTE) model. The total emission listed in table 3 is therefore the measured excess referred to the theoretical value for a NLTE model, expressed in units of the expected

TABLE 3

TOTAL FLUXES IN H^- FREE-BOUND CONTINUUM

Star	$\int H_\nu d\nu$ (10^{10} ergs s^{-1} cm^{-2} sr^{-1})	$\int \mathcal{F}_\nu d\nu$ (10^{-23} ergs s^{-1} cm^{-2})
Oo 2284	1.9	4.8
HD 14422	1.8	8.0
MWC 445	2.2	6.7
MWC 43	3.2	7.4
HD 14605	4.3	6.7
Hi 263	3.2	5.1
MWC 449	3.8	5.6
MWC 448	4.4	5.0
Mean	3.1	6.2

emission into all solid angles by a 1-cm^2 stellar surface element. Since the emission almost certainly originates in a shell many stellar radii above the photosphere, the simple physical interpretation of the numbers no longer applies. The numbers of table 3 are substantially smaller than the fluxes given by Schild (1972), which were referred to a model by Carbon and Gingerich (1969). The difference arises principally from the units in which the fluxes are given; the Mihalas absolute fluxes (Eddington fluxes H_ν) are one-fourth the SAO fluxes F_ν, which are related to the total luminosity through $L_\nu = 4\pi R^2(\pi F_\nu) = 4\pi R^2(4\pi H_\nu)$. Small additional differences between the Mihalas and the SAO models cause differences between the predicted monochromatic fluxes in the visible spectral region; these differences are in the sense that, for given atmosphere parameters, the Mihalas model is about 10 percent fainter at V than is the SAO model.

Because the above fluxes are referred to the photosphere of a star, whereas the H^- free-bound emission presumably arises in an extensive shell surrounding the star, it may be more practical to express the emission in terms of total power received at the Earth. This quantity is given in table 3 and is based on the Oke and Schild (1970) calibration of the absolute magnitude scale, together with the scanner data with reddening corrections applied for individual stars as noted in Appendix B. The mean H^- bound-free excess is 6.2×10^{-23} ergs s^{-1} cm^{-2}, and the values for individual stars again show surprisingly little variation about the mean. This is consistent with the appearance of the spectra noted in Schild (1966) and will be commented on in the concluding section.

We note that the ratios of the H^- free-bound excesses for the eight stars are not preserved between the two columns of table 3. This is because the numbers in the second column are based on comparison with a single model atmosphere, whereas those in the third column are based on the apparent visual magnitudes and the $B - V$ color excesses determined as noted above.

Finally, the total amount of energy emitted in the H^- free-bound continuum is a small fraction of the total luminosity of the star. Adopting an effective temperature of 25,000° K for the Perseus extreme Be stars, we compute an integrated flux at the star of $\sim 10^{13}$ ergs s^{-1} cm^{-2}. The H^- bound-free contribution is smaller by a factor of approximately 500.

V. EXTREME Be STARS IN OTHER CLUSTERS

To confirm the suggestion made previously (Schild 1966) that the extreme Be stars are in the secondary core-contraction phase, it would be useful to identify candidates in other clusters.[1] As has been

[1] The spectral types reported in Schild (1966) were derived when the system of spectral classification of B stars was being reexamined, and the possibility of systematic differences with the 1953 MK system (Johnson and Morgan 1953) was being allowed for with the use of lowercase Roman numerals for the luminosity classes. It has since been found that there are no systematic differences, and the luminosity-class designations should be changed to uppercase.

previously noted, χ Oph is a candidate of particular interest since it is a member of the Scorpio-Centaurus association and is relatively bright. Furthermore, it is in the position above the main sequence noted for the Perseus extreme Be stars (see Garrison [1967] for an H-R diagram of the Scorpio-Centaurus association). However, χ Oph may not be a typical extreme Be star, since as noted by Burbidge (1952), its hydrogen emission lines appear to be formed in an optically thick region.

Three other candidates in clusters can be recognized. Star Walker No. 65 in NGC 6530 is particularly interesting, because it is the one Be star in the cluster given a B0 IVpne classification by Hiltner, Morgan, and Neff (1965). Their H-R diagram shows the star to be above the main sequence, in the place expected for core-contraction stars. Fortunately, Walker No. 65 is near the cluster center, and its interstellar reddening is reasonably well defined. Furthermore, broad-band photometry from 0.33–3.5 μ has been published for this star by Johnson (1967*a*, *b*) who attempted to interpret the data in terms of dust absorption.

Johnson's (1967*a*) broad-band photometry has been reanalyzed without the use of spectrum-color relations inapplicable to extreme Be stars. First, a reddening map of NGC 6530 was prepared from the color excesses derived by Hiltner *et al.* (1965) from spectral types and *UBV* photometry of the other cluster stars. A color excess of $E_{B-V} = 0.33 \pm 0.03$ was derived; it was then used with the Whiteoak (1966) reddening curve to deredden the fluxes of Walker No. 65. The dereddened colors were compared with Johnson's (1966) intrinsic colors for the spectral type, and the infrared excesses determined. These infrared excesses were put in absolute units by the use of Johnson's (1966) calibration of the broad-band photometry and a 30,000° K, $\log g = 3.0$ NLTE model of Mihalas (1972). Uncertainties in the reddening are expected to be unimportant, and the results are essentially independent of the model chosen. The absolute calibration of Johnson is systematically different from the Oke and Schild (1970) calibration, but the differences are small and unimportant for the present work.

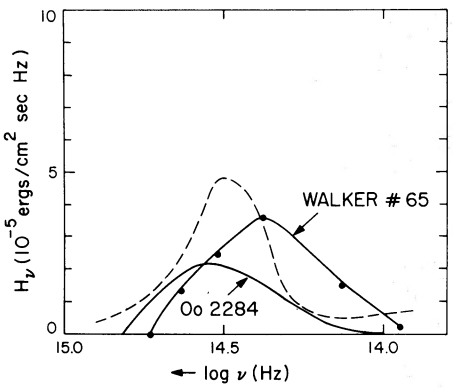

FIG. 3.—Infrared excess of Walker No. 65 in NGC 6530, from broad-band photometry. Shown in comparison are excess curves for Oo 2284 in χ Per and the 3000° K theoretical curve (*dashed line*).

The infrared excess for Walker No. 65 is shown in figure 3, together with the typical Perseus extreme Be star Oo 2284 and the theoretical curve of Milkey and Dyck (1973). The shapes of the two observed curves are similar, but the excess of Walker No. 65 appears to be displaced to longer wavelengths. Both observed curves are broader than the theoretical curve; the last, however, was drawn from arbitrarily chosen parameters.

Two other clusters containing an extreme Be star are NGC 6871 and NGC 6913. The cluster mean $B - V$ color excess is exceeded by 0.22 mag by the extreme Be star in NGC 6871 and by 0.10 mag for NGC 6913. Both candidate stars have spectral classifications indicating strong peculiarity (B0pe and Bpe), and both clusters are approximately the age of χ Per and NGC 6530, as indicated by their turnups at spectral type B0.

Of particular interest for our understanding of the evolutionary status of extreme Be stars are the H-R diagrams of NGC 6871 and NGC 6913 shown in figure 4. Both clusters contain supergiants, and H-R diagrams for both are available from the data of Hoag and Applequist (1965). If we assume that the $B - V$ colors of the extreme Be stars are affected by the H^- free-bound emission and correct the observed visual magnitudes by the cluster mean $B - V$ excesses, we find the extreme Be stars among the luminosity class III giants. This is the region of the H-R diagram where stars in the secondary core-contraction phase are found, consistent with the interpretation to be made below.

In this context, the spectroscopic observations of Be stars in NGC 330 in the SMC (Feast 1972) are particularly enlightening. The Be stars were found to be concentrated in the same region of the H-R diagram as was found for χ Per, and several stars having very strong Hα emission, probably extreme Be stars, were recognized. Feast has also noted several Be stars barely above the zero-age main sequence (ZAMS),

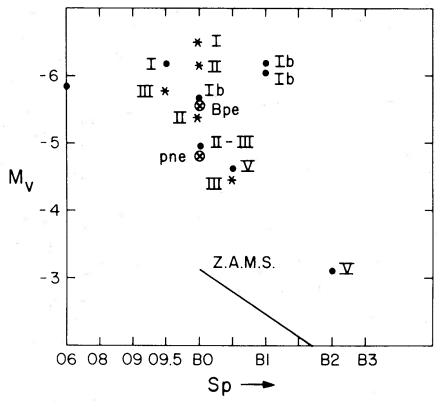

FIG. 4.—Composite H-R diagram for MGC 6871 (*dots*) and NGC 6913 (*asterisks*) to show the location of the extreme Be stars among the giants. For the distance moduli given by Hoag and Applequist (1965), the ZAMS is shown. The extreme Be stars are shown as circles with crosses.

confirming the result first obtained for χ Per that not all Be stars are in the secondary core-contraction stage.

VI. THE EVOLUTIONARY STATUS OF EXTREME Be STARS

Several aspects of the extreme Be stars can be reviewed at this point:

a) Evidence in support of the suggestion of Schild (1966) that the χ Per extreme Be stars are post–main-sequence objects in the region of the H-R diagram where secondary core contraction occurs is extended to three more young clusters.

b) Many of the spectroscopic properties of extreme Be stars can be explained by the presence of a very large cloud of gas that provides emission lines and excess continuum radiation in the near-infrared.

c) The most recent calculations of rotating evolving B stars (Sackmann and Anand 1970) continue to show the result first noted by Crampin and Hoyle (1960) that rotating evolving B stars have some tendency to lose mass in their evolution away from the main sequence and a very strong tendency to do so during the secondary core-contraction stage.

d) Lucy and Solomon (1970) have shown that stars near the main sequence with $\log T_{\rm eff}(^\circ\,{\rm K}) = 4.38$–$4.44$ have a strong tendency to lose mass owing to momentum transfer associated with ultraviolet absorption at frequencies of resonance lines of light elements. The effective temperatures correspond to those of spectral types B0.5–B1.

e) In clusters containing extreme Be stars, spectral types of the cluster members at turnup and of the extreme Be stars themselves are B0–B1.5, which is barely larger than and well centered on the range noted in (*d*) above.

We suggest that extreme Be stars are objects in the secondary contraction phase of post–main-sequence evolution and that this explains their locations above the main sequence in the cluster H-R diagrams. We further suggest that most ordinary Be stars are in the early post–main-sequence stage of evolution and that the extreme Be stars develop very extensive shells in response to the momentum transfer resulting from absorption in resonance lines, as proposed by Lucy and Solomon (1970). The connection of the Be phenomenon with Lucy and Solomon's mechanism is supported by the coincidence of the predicted temperature of the maximum effect and the observed spectral types of stars with H^- free-bound emission. In this connection, we mention the little-known fact that hydrogen emission is rarely observed in stars near the main sequence at spectral types O8–O9.5, consistent with Lucy and Solomon's result that the resonance absorption is relatively unimportant for those temperatures. Unfortunately, the one cluster rich in O9–O9.5 stars, NGC 6231, is poor in emission-line stars but, interestingly enough, rich in binaries. It would be important to confirm the observation of Schild (1966) that the extreme Be stars in Perseus, as seen at low dispersion, have their Hγ emission component blueshifted relative to the absorption. If the effect is present at Hβ and Hα, it would lend further support to the resonance-absorption hypothesis.

Another group identified as extreme Be stars are the objects formerly called pole-on stars (Schild 1973). They have similar hydrogen line profiles, helium absorption profiles, and large infrared excesses and, by comparison with the Perseus stars, are inferred to be also in the secondary core-contraction phase. However, the former pole-on stars do not appear to have veiled He I lines, and at least one of them, β Psc, does not have the $B - V$ excess indicative of the H^- free-bound emission. These stars are systematically of later spectral type than are the Perseus extreme Be stars, which probably accounts for their different properties.

While the latest far-ultraviolet spectra of early B giants and dwarfs by Morton, Jenkins, and Macy (1972) and Morton *et al.* (1972) show no evidence for stellar winds generated by momentum transfer associated with resonance-line absorption as suggested by Lucy and Solomon (1970), the process may contribute to the pressure support of the enormous envelopes apparently necessary to provide the observed strength of H^- free-bound emission in the Perseus extreme Be stars. Cassinelli and Castor (1973) have emphasized the need to have finite absorptive opacity for the flow to become supersonic. Further studies at all wavelengths of the continuum radiation of Be stars are essential for the understanding of the formation and dynamics of the Be star atmosphere.

We would like to thank our colleague, J. Rand Baldwin, for several discussions and a critical reading of this manuscript. For substantial technical assistance in the operation of our spectrometer and infrared equipment at Mount Hopkins, we thank B. van't Sant.

APPENDIX A

ENERGY DISTRIBUTIONS OF ORDINARY Be STARS

Few energy distributions of Be stars are available in the current literature, and the nature of the Balmer discontinuity and Paschen continuum is difficult to infer from broad-band photometry. We therefore present data for 10 Be stars to show that most Be stars do not have the near-infrared excess emission and that most do have approximately the normal Balmer discontinuity for their spectral type.

Ten Be stars of spectral type B1 Ve to B3 Ve were selected from the catalog of Lesh (1968). Spectral types of these stars are all recently derived and are of the highest quality. Furthermore, this selection criterion favors the most pronounced Be stars, since many weak Be stars have no Hβ emission.

For each of the 10 stars, a single observation made between 1968 September 20–23 on the Mount Wilson 100-inch (2.5-m) telescope is available. Time did not permit the observations to be repeated then, and repetition at a later date would not permit favorable comparison, since most Be stars appear to be some-

TABLE A1

DATA FOR FIELD Be STARS

HD	HR	SP	V	$B-V$	E_{B-V}	$m_{3636}-m_{4255}$	T_e (° K)	$\theta_{\rm eff}$
164284.....	6712	B2 Vel	4.69	−0.05	0.19	+0.01	23,400	0.215
168797.....	6873	B3 Vel*	6.11	−0.03	0.17	+0.30	18,200	0.28
183362.....	7403	B3 Vel+	6.32	−0.14	0.16	+0.08	22,000	0.23
187567.....	7554	B2.5 IVel+	6.52	−0.08	0.14	+0.08	22,000	0.23
194335.....	7807	B2 Veln†	5.88	−0.20	0.04	+0.04	23,000	0.22
197419.....	7927	B2 IV–Ve3	6.68	−0.16	0.08	+0.29	18,600	0.27
200120.....	8047	B1.5 Ve2nn†	4.79	−0.07	0.18	...	...	...
202904.....	8146	B2 Vel+†	4.28	−0.08	0.16	+0.04	23,000	0.22
212571.....	8539	B1 Vel*	4.68	−0.03	0.23	...	...	...
214168.....	8603	B1 Vel*	5.74	−0.14	0.12	−0.05	25,000	0.20

* Variable radial velocity. † Spectroscopic binary.

what variable. Observations of other objects made during the same run show the nights to have been of the highest photometric quality. Although errors cannot be determined internally from a comparison of multiple observations of the stars, external error indicators, such as the agreement of observations of standards, show that the usual photometric accuracy, i.e., $\sim \pm 0.02$ mag in the visible and ± 0.03 mag in the ultraviolet, probably is realized. Pulse-counting electronics were used, and at least 10^4 counts were obtained at each wavelength, except at 6000 Å for a few of the stars. A 50 Å bandpass and 10-s integration were used. All observations have been reduced to the system of Oke and Schild (1970).

The stars observed are listed in table A1, where other data for the stars are also collected. The spectral types and *UBV* photometry have all been taken from Lesh (1968). The reddening law of Whiteoak (1966) was used to deredden the stars according to the $B-V$ excesses listed in table A1.

The observed fluxes in the form $-2.5 \log F_\nu + C$, with no reddening corrections applied, are listed in table A2. The reddening-corrected fluxes are not tabulated, but are shown graphically in figure 5, where the observed continuum of the B2 III unreddened field star β Cep from Schild, Peterson, and Oke (1971) is shown for comparison. For most stars, the slope of the Balmer continuum agrees well with that of β Cep, which suggests that the reddening law and reddening corrections applied are proper. Moreover, the temperatures indicated by the slope of the Paschen continuum and those by the Balmer discontinuity are in substantial agreement, as has been found for β Cep (Schild *et al.* 1971). There is some suggestion that the reddening correction applied to HR 7403 is slightly too large. The correction applied to HR 7554 is evidently too small, and a much better fit to β Cep results if the $B-V$ excess is taken to be 0.22. Such a large excess, if combined with the star's observed $B-V$ color of −0.08 (Lesh 1968) or −0.10 (Mendoza 1958), would give an intrinsic color of about $B-V=-0.31$; such a color is inconsistent with the star's Balmer jump and line spectrum. Therefore, the star's Balmer jump has been computed for an assumed reddening correction as illustrated. It is, of course, possible that the star's energy distribution has changed.

An apparent effective temperature can be derived from a measurement of the Balmer discontinuity to permit comparison of the apparent (effective temperature, spectral type)-relation with that derived for field stars (Schild *et al.* 1971). This has been done by the following procedure. Smooth curves were drawn through the points shown in figure 5, and the magnitude difference $m_{3636}-m_{4255}$ was read from the smoothed curves. This difference was then entered into figure 1 of Schild *et al.* (1971), from which effective temperatures were read. The magnitude differences and effective temperatures are listed in table A1.

This procedure encountered no difficulty for the majority of program stars, for which it is estimated that the error of the magnitude difference $m_{3636}-m_{4255}$ was only ± 0.03, which results in an error in effective temperature of 3 percent. Systematic errors in the models on which this work is based, and in absolute calibration, are likely to be of this amount or greater. Moreover, the interpretation of these apparent effective temperatures is not yet clear.

The star HR 7554 was difficult to match to the model continuum because of the uncertainty of its reddening correction, as noted above. The effective temperature listed in table A1 refers to a best fit to the continuum unreddened according to $E_{B-V}=0.14$. If the higher reddening value, $E_{B-V}=0.22$, is assumed, an effective temperature approximately 1000° higher is found.

For two stars listed in table A1, no effective temperatures have been derived, because the Balmer discontinuities are vanishingly small and inconsistent with the line spectra. It is a shortcoming of this investigation that spectra and energy distributions were not obtained in the same year, since many of the Be stars are known to be spectrum variables and the energy distributions are likely to be variable also. A further complication is that one of the stars with small Balmer discontinuity is a spectroscopic binary and the other exhibits variable radial velocity.

The (effective temperature, spectral type)-relation for the Be stars is compared with that for field B stars in figure 6. The solid curve in figure 6 was obtained by

TABLE A2

ENERGY DISTRIBUTIONS F_ν FOR FIELD Be STARS (magnitudes)

	HR									
λ	6712	6873	7403	7554	7807	7927	8047	8146	8539	8603
3300.....	4.42	6.20	6.16	6.21	5.46	6.46	4.24	4.27	4.16	5.28
3390.....	4.46	6.20	6.20	6.20	5.51	6.52	4.28	4.28	4.19	5.30
3509.....	4.46	6.26	6.20	6.22	5.53	6.58	4.30	4.27	4.20	5.37
3571.....	4.44	6.24	6.22	6.21	5.56	6.59	4.33	4.29	4.29	5.38
3636.....	4.46	6.26	6.22	6.22	5.59	6.62	4.33	4.30	4.24	5.41
3704.....	4.48	6.17	6.24	6.22	5.58	...	4.37	4.35	4.25	...
4055.....	4.34	5.83	5.99	6.04	5.47	6.20	4.38	4.13	4.35	5.31
4195.....	4.36	5.86	6.03	6.07	5.52	6.27	4.39	4.16	4.36	5.36
4233.....	4.36	5.89	6.04	6.08	5.54	6.27	4.41	4.17	4.35	5.37
4420.....	4.39	5.94	6.10	6.14	5.60	6.34	4.45	4.23	4.39	5.44
4582.....	4.39	5.93	6.11	6.11	5.61	6.37	4.43	4.23	4.35	5.44
4810.....	4.44	5.96	6.19	6.18	5.71	6.43	4.49	4.31	4.46	5.50
4975.....	4.52	6.02	6.24	6.21	5.76	6.50	4.54	4.37	4.49	5.56
5100.....	4.52	6.03	6.27	6.23	5.80	6.55	4.55	4.40	4.55	5.58
5250.....	4.52	6.06	6.29	6.23	5.84	6.56	4.56	4.42	4.53	5.62
5490.....	4.55	6.09	6.34	6.25	5.91	6.63	4.60	4.47	4.57	5.67
5625.....	4.56	6.09	6.38	6.29	5.93	6.67	4.62	4.50	4.58	5.72
5800.....	4.58	6.15	6.43	6.31	6.01	6.73	4.67	4.55	4.58	5.77
6000.....	4.64	6.18	6.45	6.36	6.04	6.76	4.72	4.56	4.57	5.80

converting the smooth (Q, $\theta_{\rm eff}$)-relation of figure 3 in Schild *et al.* (1971) by the use of Johnson and Morgan's (1953) (mean Q, spectral type)-relation. The direct plotting of spectral types in figure 6 permits some estimate of the effects of classifying in discrete "boxes."

It can be seen from figure 6 that the apparent effective-temperature relation for field stars fits the Be stars quite well. There is some evidence that the energy distributions for the Be stars indicate slightly higher apparent effective temperatures. The difference, however, is small; the displacement of the mean curve for ordinary B stars to obtain a best fit to the data for the

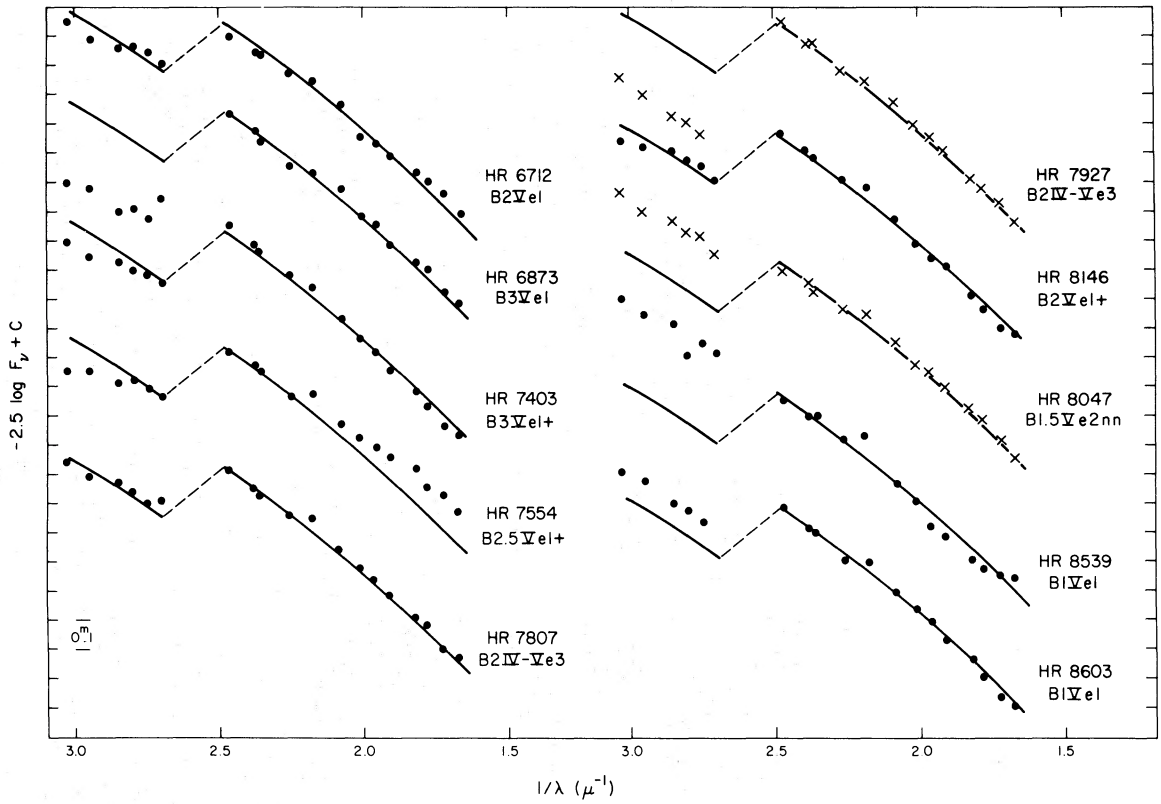

FIG. 5.—Dereddened energy distributions of Be stars, compared to the energy distribution of β Cep (B2 III, *solid curve*)

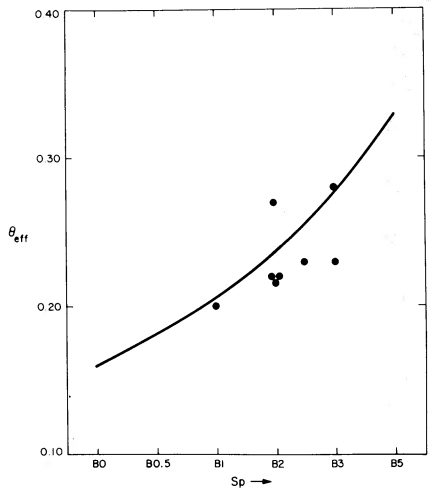

FIG. 6.—The (spectral type, θ_{eff})-relation for Be stars. The solid curve is the mean relation for field B stars found by Schild *et al.* (1971).

Be stars amounts to less than half an ordinary spectral subdivision.

Two stars depart significantly from the mean relation. HR 7403 has too small a Balmer discontinuity for its spectral type of B3. An earlier spectral classification of B2 by Mendoza (1958) is more consistent with the energy distribution. HR 7927 has too large a Balmer discontinuity for its spectral type of B2, but its previous classification by Mendoza (B2:) is consistent with that of Lesh (1968). Very strong emission is indicated by Lesh's e3 emission classification for this star.

Four conclusions can be drawn:

a) Ordinary treatment of $B - V$ colors and spectral types of Be stars appears to be justified in the majority of cases, on the ground that it yields energy distributions similar to those found for nonemission B stars.

b) The slope of the Paschen continuum from 4000–6000 Å for most Be stars appears to be compatible with their Balmer jumps on the absolute calibration system of Oke and Schild (1970). A similar agreement is found for the field B stars (Schild *et al.* 1971).

c) Apparent effective temperatures of Be stars, derived by comparing measured Balmer discontinuities with model atmospheres, are in close agreement with the scale for ordinary B stars found by Schild *et al.* (1971). The departure is in the sense that slightly higher apparent effective temperatures are indicated for the Be stars at the respective spectral types. The significance of the departure is doubtful and should be investigated by more extensive data.

d) Some Be stars appear to have energy distributions not at all consistent with their line spectra.

APPENDIX B

NOTES ON PARTICULAR EXTREME Be STARS

HD 14422.—The 1971 energy distribution shows the same features as one measured in 1968 and reported in Schild (1971). However, the infrared data of 1972 January 10 are ~0.3 mag brighter than the fall 1970 data. We believe the star's infrared brightness is variable. The 1971 scan and the 1972 January infrared observations have been used in the present paper, with a $B - V$ color excess of 0.57.

HD 14605.—The 1971 energy distribution is used with 1972 January infrared data. The latter are about 0.1 mag fainter than the 1970 infrared data at both 1.6 and 2.2 μ with insufficient data at 3.5 μ. We believe the star is probably variable.

Hi 263.—The 1968 Mount Wilson scans are in excellent agreement with the 1971 Mount Hopkins data. However, the only infrared data available are from the fall of 1970.

MWC 42.—The 1968 Mount Wilson scans are in excellent agreement with the 1971 Mount Hopkins data. The two sets of infrared data agree to within the errors.

MWC 445.—Only Mount Hopkins energy distributions are available, and the infrared data of 1970 agree with the 1972 data to within the errors.

MWC 448.—Only Mount Hopkins scans from 1971 and only 1970 infrared observations are available.

MWC 449.—Only 1971 energy distributions, and no infrared data, are available. The color excess of $E_{B-V} = 0.57$ indicated by the reddening map of the association did not give a satisfactory fit in the 4200 Å region, and an $E_{B-V} = 0.70$ was adopted. The total flux for MWC 449 was derived by fitting the Hi 263 infrared data, which are very average for the extreme Be stars.

Oo 2284.—Only 1971 energy distributions and 1972 infrared data are available for this star. Because Oo 2284 is in the nucleus of χ Per, where reddening has been well determined by Crawford *et al.* (1970), its infrared continuum excess is especially well defined.

APPENDIX C

THE REDDENING LAW IN THE ULTRAVIOLET

The standard reddening law used for the Perseus stars (Whiteoak 1966; table 7) is based on a comparison of measured energy distributions with models of hot stars. It is, therefore, dependent on absolute calibration. Unfortunately, the Whiteoak results are given only to 0.345 μ, whereas energy distributions are currently measured routinely to 0.320 μ at good photometric sites.

To update and extend to shorter wavelength the Whiteoak curve, we have made a new comparison of the fluxes of reddened stars with models. The absolute calibration of Oke and Schild (1970) was used to compare the newly observed fluxes of HD 199216 (B1 II, $E_{B-V} = 0.72$) with an ultraviolet line-blanketed model at $T_{\rm eff} = 26{,}000°$ K, $\log g = 4.0$ (Van Citters and Morton 1970). Because the gravity of the model is too high for the star, we have normalized our reddening curve to Whiteoak's at the longest ultraviolet wavelengths, so we only require the model atmosphere and the star to have the same *slope* in the Balmer continuum. Because of the large reddening of HD 199216, this procedure is probably adequate for correcting stars with $E_{B-V} \leq 0.50$, but may lead to errors of a few percent for greater reddening. The uncertainty inherent in extrapolating the absolute calibration to 0.32 μ probably exceeds the error introduced by comparing with an atmosphere of higher surface gravity.

In table C1, we list our newly derived reddening law for the ultraviolet and compare it at four wavelengths with Whiteoak's (1966) results. While this reddening law should be improved by comparing energy distributions of highly reddened and unreddened stars of the same spectral types in order to eliminate the absolute-calibration uncertainty, the present results are adequate for the purposes of this paper. The numbers in table C1 are normalized in the same way as the data in table 7 of Whiteoak (i.e., to a color excess of 0.50 mag between $\lambda\lambda$4464 and 5556).

TABLE C1

WAVELENGTH DEPENDENCE OF EXTINCTION

λ	$1/\lambda$	Whiteoak (1966)	Present
3200	3.12	...	1.25
3250	3.08	...	1.18
3300	3.03	...	1.12
3350	2.99	...	1.09
3400	2.94	...	1.05
3450	2.90	1.01	1.02
3500	2.85	0.98	0.98
3571	2.80	0.95	0.95
3636	2.75	0.91	0.92

REFERENCES

Burbidge, E. M. 1952, *Ap. J.*, **115**, 418.
Carbon, D. F., and Gingerich, O. 1969, in *Theory and Observation of Normal Stellar Atmospheres*, ed. O. Gingerich (Cambridge: MIT Press), p. 377.
Cassinelli, J. P., and Castor, J. I. 1973, *Ap. J.*, **179**, 189.
Crampin, J., and Hoyle, F. 1960, *M.N.R.A.S.*, **120**, 33.
Crawford, D. L., Glaspey, J. W., and Perry, C. L. 1970, *A.J.*, **75**, 822.
Feast, M. W. 1972, *M.N.R.A.S.*, **159**, 113.
Garrison, R. F. 1967, *Ap. J.*, **147**, 1003.
Hiltner, W. A., Morgan, W. W., and Neff, J. S. 1965, *Ap. J.*, **141**, 183.
Hoag, A. A., and Applequist, L. 1965, *Ap. J. Suppl.*, **12**, 215.
Johnson, H. L. 1966, *Ann. Rev. Astr. and Ap.*, **4**, 193.
———. 1967*a*, *Ap. J.*, **147**, 912.
———. 1967*b*, *Ap. J.* (*Letters*), **150**, L39.
Johnson, H. L., and Morgan, W. W. 1953, *Ap. J.*, **117**, 313.
Lesh, J. 1968, *Ap. J. Suppl.*, **17**, 371.
Lucy, L. B., and Solomon, P. M. 1970, *Ap. J.*, **159**, 879.
Mendoza, V. E. 1958, *Ap. J.*, **128**, 207.
Mihalas, D. 1972, NCAR Tech. Note No. NCAR-TN/STR-76.
Milkey, R. W., and Dyck, H. M. 1973, *Ap. J.*, **181**, 833.
Morton, D. C., Jenkins, E. B., and Macy, W. W. 1972, *Ap. J.*, **177**, 235.
Morton, D. C., Jenkins, E. B., Matilsky, T. A., and York, D. G. 1972, *Ap. J.*, **177**, 219.
Oke, J. B., and Schild, R. E. 1970, *Ap. J.*, **161**, 1015.
Sackmann, I. J., and Anand, S. P. S. 1970, *Ap. J.*, **162**, 105.
Schild, R. E. 1966, *Ap. J.*, **146**, 142.
———. 1972, *Mém. Soc. Roy. Sci. Liège*, 6th Series, **3**, 295.
———. 1973, *Ap. J.*, **179**, 221.
Schild, R. E., Peterson, D. M., and Oke, J. B. 1971, *Ap. J.*, **166**, 95.
Van Citters, G. W., and Morton, D. C. 1970, *Ap. J.*, **161**, 695.
Whiteoak, J. 1966, *Ap. J.*, **144**, 305.
Wilson, W. J., Schwartz, P. R., Neugebauer, G., Harvey, P. M. and Becklin, E. E. 1972, *Ap. J.*, **177**, 523.